

Discussion on a Class of Model-Free Adaptive Control for Multivariable Systems

Feilong Zhang

Abstract—The model-free adaptive control (MFAC) law is a promising method in applications. We analyzed model-free adaptive control (MFAC) law through closed-loop function to widen its application range.

Index Terms—model-free adaptive control.

I. INTRODUCTION

Tremendous amount of works concerning MFAC have been published in this decade. [a] has discussed some problems in [1]-[2] which designed MFAC in single-input single-output systems. Similar to [a], we have analyzed several problems in multiple-input multiple-output (MIMO) systems as follows.

i) The leading coefficient matrix of control input vector is restricted to a special kind of diagonally dominant matrix with the unchangeable sign of the diagonal elements [4]-[5]. We show that the previous assumption turns out to be restrictive and can be extended in this paper and [b]. In addition, the pseudo orders of the current equivalent dynamic linearization model and MFAC are limited within $1 \leq L_y \leq n_y$ and $1 \leq L_u \leq n_u$. However, it seems that the most important case is $L_y = n_y + 1$ and $L_u = n_u + 1$ with the purpose of pseudo Jacobian matrix acting as the real Jacobian matrix. To this end, we extend the range into $0 \leq L_y$ and $1 \leq L_u$.

ii) The static error of the unit-ramp response of the system is eliminated by choosing $\lambda = 0$ when $M_u \geq M_y$, which is proved in this brief. This conclusion differs from [1]-[5] which showed that the tracking error of the system controlled by MFAC converges to zero on the condition that λ is large enough. Moreover, [a] shows the reason why the tracking error of the step response of the system controlled by current MFAC converges to zero, which is not in relation to λ and should be attributed to the fact that the current MFAC inherently contains an integrator.

iii) The current works about MFAC method in MIMO systems take the norm of the inverse matrix in the controller design with the purpose of analyzing the system stability through the contraction mapping method. Nevertheless, this will lead to the inaccurate inputs and outputs coupling information in the controller.

iv) The notion of model-free presented for nonlinear systems in [1]-[5] is not straightforward for operating engineers to understand appropriately and to master its essence. [b] analyzes

this class of controller in linear deterministic finite-dimensional systems in simulations to exhibit its working principle and discuss the nature of this kind of adaptive controller. In this brief, the MFAC is applied in the robotic system to demonstrate its effectiveness, and meanwhile to exhibit an appropriate and successful application in the nonlinear system.

In this brief, the full-form equivalent-dynamic-linearization model is extended to a general form with the pseudo Jacobian matrix (PJM) not restricted by the special diagonally dominant matrix assumption anymore and the number of input variables and output variables of the system are allowed to be different. As the consequence, the MFAC can be more widely applied. This is all possible because we have analyzed the system performance by the closed-loop system equations and the static error analysis rather than by the current contraction mapping method. Along with this, we have reached the conclusion that the static error of the system following the reference $k^n \mathbf{I} (n \geq 1)$ is positively correlated with λ in this brief, [a] and [c]. These imply that the conclusion about the convergence of tracking error in current works may not always be reasonable.

Only when we study the MFAC in a reasonable way, can we apply this method in a proper way, and this is one of main motivations in this brief. At last, we have used iterative MFAC to design a simple yet useful robotic controller which shows an excellent performance.

II. EQUIVALENT DYNAMIC LINEARIZATION MODEL FOR MULTIVARIABLE SYSTEMS

This section presents a kind of full form equivalent dynamic linearization model for a family of multivariable system, which is used for MFAC controller design and analysis in next section.

The MIMO nonlinear system is given as:

$$\mathbf{y}(k+1) = \mathbf{f}(\mathbf{y}(k), \dots, \mathbf{y}(k-n_y), \mathbf{u}(k), \dots, \mathbf{u}(k-n_u)) \quad (1)$$

where $\mathbf{f}(\dots) = [f_1(\dots), \dots, f_m(\dots)]^T \in \mathbf{R}^m$ is assumed to be the nonlinear vector-valued function; $\mathbf{u}(k)$ and $\mathbf{y}(k)$ are the input vector and output vector of the system, respectively; $n_y + 1, n_u + 1 \in \mathbf{Z}$ are the corresponding orders. The dimensions of $\mathbf{y}(k)$ and $\mathbf{u}(k)$ are M_y and M_u , respectively.

Assumption 1: The partial derivatives of $\mathbf{f}(\dots)$ with respect to all input vectors and output vectors are continuous.

Theorem 1: Given system (1) satisfying *Assumptions 1*, if $\Delta \mathbf{h}(k) \neq 0$, $0 \leq L_y$, $1 \leq L_u$, there must exist a matrix $\phi_l^T(k)$ named pseudo Jacobian matrix, and (1) can be transformed into the following model:

Manuscript received Dec 3, 2020. This work was supported in part by the xxxxxxxx

Feilong Zhang is with the State Key Laboratory of Robotics, Shenyang Institute of Automation, Chinese Academy of Sciences, Shenyang 110016, China (e-mail: zhangfeilong@sia.cn).

$$\Delta \mathbf{y}(k+1) = \Phi_L^T(k) \Delta \mathbf{h}(k) \quad (2)$$

where

$$\begin{aligned} \Phi_L^T(k) &= [\Phi_{Ly}^T(k)_{My \times (Ly+My)}, \Phi_{Lu}^T(k)_{My \times (Lu+Mu)}] \\ &= [\Phi_1(k), \dots, \Phi_{Ly}(k), \Phi_{Ly+1}(k), \dots, \Phi_{Ly+Lu}(k)]^T, \\ \Phi_i(k) &= \begin{bmatrix} \phi_{11i}(k) & \phi_{12i}(k) & \dots & \phi_{1mi}(k) \\ \phi_{21i}(k) & \phi_{22i}(k) & \dots & \phi_{2mi}(k) \\ \vdots & \vdots & \ddots & \vdots \\ \phi_{m1i}(k) & \phi_{m2i}(k) & \dots & \phi_{mmi}(k) \end{bmatrix} \in \mathbf{R}^{My \times My}, \end{aligned}$$

$i=1, \dots, Ly$, and $\Phi_i(k) \in \mathbf{R}^{My \times Mu}$, $i=Ly+1, \dots, Ly+Lu$; $m=My$, and

$$\Delta \mathbf{h}(k) = \begin{bmatrix} \Delta \mathbf{Y}(k) \\ \Delta \mathbf{U}(k) \end{bmatrix} = [\Delta \mathbf{y}^T(k), \dots, \Delta \mathbf{y}^T(k-L_y+1), \Delta \mathbf{u}^T(k), \dots, \Delta \mathbf{u}^T(k-L_u+1)]^T$$

is a vector

that contains the increment of control input vectors and the increment of system output vectors within the time window $[k-L_u+1, k]$ and $[k-L_y+1, k]$, respectively. The integers L_y ($0 \leq L_y$) and L_u ($1 \leq L_u$) are named pseudo orders of the system.

Remark 1: [3] gives the proof of the *Theorem 1* in the case of $1 \leq L_y \leq n_y$, $1 \leq L_u \leq n_u$ and we further prove *Theorem 1* for the orders $0 \leq L_y$ and $1 \leq L_u$ in Appendix.

We prefer $L_y=n_y+1$ and $L_u=n_u+1$ in applications if n_y and n_u can be obtained. Otherwise, we usually choose the proper L_y and L_u that satisfy $n_y+1 \leq L_y$ and $n_u+1 \leq L_u$ in adaptive control. One reason is that the online estimated coefficient matrices of redundant items $\Delta \mathbf{y}(k-n_y-1), \dots, \Delta \mathbf{y}(k-L_y+1)$ and $\Delta \mathbf{u}(k-n_u-1), \dots, \Delta \mathbf{u}(k-L_u+1)$ might be close to zero matrix. In the meantime the estimated coefficients of $\Delta \mathbf{y}(k), \dots, \Delta \mathbf{y}(k-n_y)$ and $\Delta \mathbf{u}(k), \dots, \Delta \mathbf{u}(k-n_u)$ will be more close to the true values compared to $0 \leq L_y \leq n_y$ and $1 \leq L_u \leq n_u$.

III. FFDL-MFAC DESIGN AND STABILITY ANALYSIS

This section provides the design and stability analysis methods for MFAC.

A. Design of Model-Free Adaptive Control

We rewrite (2) into (3).

$$\mathbf{y}(k+1) = \mathbf{y}(k) + \Phi_L^T(k) \Delta \mathbf{h}(k) \quad (3)$$

A control input criterion function is given as:

$$J = [\mathbf{y}^*(k+1) - \mathbf{y}(k+1)]^T [\mathbf{y}^*(k+1) - \mathbf{y}(k+1)] + \Delta \mathbf{u}^T(k) \lambda \Delta \mathbf{u}(k) \quad (4)$$

where $\lambda = \text{diag}(\lambda_1, \dots, \lambda_{Mu})$ is the weighted diagonal matrix and λ_i ($i=1, \dots, M_u$) are equal to λ for the system analysis, according to [3]; $\mathbf{y}^*(k+1) = [\mathbf{y}_1^*(k+1), \dots, \mathbf{y}_m^*(k+1)]^T$ is the desired trajectory vector.

We substitute (3) into (4) and solve the optimization condition $\partial J / \partial \Delta \mathbf{u}(k) = 0$ to have:

$$\begin{aligned} [\Phi_{Ly+1}^T(k) \Phi_{Ly+1}(k) + \lambda] \Delta \mathbf{u}(k) &= \Phi_{Ly+1}^T(k) [(\mathbf{y}^*(k+1) - \mathbf{y}(k)) \\ &\quad - \sum_{i=1}^{Ly} \Phi_i(k) \Delta \mathbf{y}(k-i+1) - \sum_{i=Ly+2}^{Ly+Lu} \Phi_i(k) \Delta \mathbf{u}(k-i+1)] \end{aligned} \quad (5)$$

Remark 2: If $\lambda = \mathbf{0}$, (5) may be the optimal solution for the tracking error control. It was also shown in [a] for SISO systems.

B. Stability Analysis of FFDL-MFAC

This section provides the performance analysis of MFAPC.

We define

$$\Phi_{Ly}(z^{-1}) = \Phi_1(k) + \dots + \Phi_{Ly}(k) z^{-Ly+1} \quad (6)$$

$$\Phi_{Lu}(z^{-1}) = \Phi_{Ly+1}(k) + \dots + \Phi_{Ly+Lu}(k) z^{-Lu+1} \quad (7)$$

where z^{-1} is the backward shift operator.

Then (2) is rewritten as

$$\Delta \mathbf{y}(k+1) = \Phi_{Ly}(z^{-1}) \Delta \mathbf{y}(k) + \Phi_{Lu}(z^{-1}) \Delta \mathbf{u}(k) \quad (8)$$

From (5)-(8), we have the following closed-loop system equations:

$$\begin{aligned} [\Delta \lambda [\mathbf{I} - z^{-1} \Phi_{Ly}(z^{-1})] + \Phi_{Lu}(z^{-1}) \Phi_{Ly+1}^T(k)] \mathbf{y}(k) \\ = \Phi_{Lu}(z^{-1}) \Phi_{Ly+1}^T(k) \mathbf{y}^*(k) \end{aligned} \quad (9)$$

$$\begin{aligned} [\Delta \lambda \mathbf{I} + \Phi_{Lu}(z^{-1}) \Phi_{Ly+1}^T(k) [\mathbf{I} - z^{-1} \Phi_{Ly}(z^{-1})]^{-1}] \Phi_{Lu}(z^{-1}) \mathbf{u}(k) \\ = \Phi_{Lu}(z^{-1}) \Phi_{Ly+1}^T(k) \mathbf{y}^*(k+1) \end{aligned} \quad (10)$$

Theorem 2: Assume

$$(1) \text{rank}[\Phi_{Ly+1}(k)] = M_y \quad (M_u \geq M_y).$$

(2) By tuning λ , we can obtain the inequation:

$$\mathbf{T} = \Delta \lambda [\mathbf{I} - z^{-1} \Phi_{Ly}(z^{-1})] + \Phi_{Lu}(z^{-1}) \Phi_{Ly+1}^T(k) \neq \mathbf{0}, \quad |z| > 1 \quad (11)$$

which determines the poles of the system. Then (5) guarantees the stability of the system according to [6]-[7].

Furthermore, the steady-state error (static error) of the unit-ramp response of the system is

$$\begin{aligned} \lim_{k \rightarrow \infty} \mathbf{e}(k) &= \lim_{\substack{z \rightarrow 1 \\ k \rightarrow \infty}} \frac{z-1}{z} (\mathbf{I} - \mathbf{T}^{-1} \Phi_{Lu}(z^{-1}) \Phi_{Ly+1}^T(k)) \frac{T_s z}{(z-1)^2} \\ &= \lim_{z \rightarrow 1} (\mathbf{T}^{-1} \lambda [\mathbf{I} - z^{-1} \Phi_{Ly}(z^{-1})]) T_s \end{aligned} \quad (12)$$

where T_s represent the sample time constant.

Evidently, the static error of ramp response of the system is proportional to λ . Furthermore, the steady-state error will be eliminated ($\lim_{k \rightarrow \infty} \mathbf{e}(k) = \mathbf{0}$) when $\lambda = \mathbf{0}$ and $M_u \geq M_y$. This noticeable result is distinct from [1]-[5] which have proved that the convergence of tracking error is guaranteed when λ is large enough. Moreover, the static error will be removed theoretically by choosing $\lambda = \mathbf{0}$, when the desired trajectory is $k^n \cdot [1, \dots, 1]_{1 \times My}^T$ ($0 < n < \infty$). We omit the proof and please refer to [a] for more details.

If $\text{rank}[\Phi_{Ly+1}(k)] = M_u$ ($M_u < M_y$), we will have the similar stability proof, however, the static error can hardly be guaranteed to be zero.

Remark 3: If the system is intensively nonlinear, the obtained $\Phi(k)$ may change apparently from time k to $k+1$, which always leads to poor system behaviors. To this end, we suggests

applying iterative MFAC controller in the way of [c]. The controller will be

$$\Delta \mathbf{u}_{(i)}(k) = \left(\boldsymbol{\lambda}_{(i)}(k) + \left[\frac{\partial \mathbf{f}}{\partial \mathbf{u}_{(i)}^T(k)} \right]_{i=i-1}^T \frac{\partial \mathbf{f}}{\partial \mathbf{u}_{(i)}^T(k)} \right)^{-1} \left(\frac{\partial \mathbf{f}}{\partial \mathbf{u}_{(i)}^T(k)} \right)^T [\mathbf{y}^*(k+1) - \mathbf{y}_{(i)}(k)] - \sum_{j=1}^{ny+1} \frac{\partial \mathbf{f}}{\partial \mathbf{y}_{(i)}^T(k-j+1)} \Delta \mathbf{y}_{(i)}(k-j+1) - \sum_{j=2}^{nu+1} \frac{\partial \mathbf{f}}{\partial \mathbf{u}_{(i)}^T(k-j+1)} \Delta \mathbf{u}_{(i)}(k-j+1) \quad (13)$$

where (i) denotes the iteration count before the control inputs are sent to the system at the time of k .

IV. SIMULATION

For more knowledge please refer to [c].

Example 1: We consider a robot with three links $l_1=5, l_2=l_3=7$ as shown in Fig. 1.

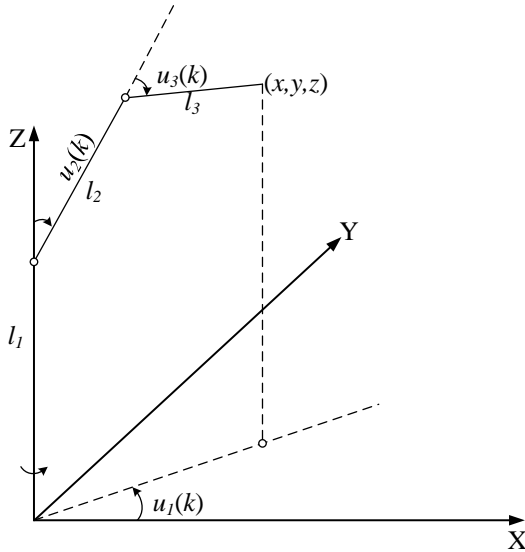


Fig. 1 Robot model

The outputs of the system are the position (x, y, z) of the robot manipulator in task space. The inputs of the system are the angles $u_1(t), u_2(t), u_3(t)$ of the robot in joint space. The system model is

$$\begin{aligned} x(k+1) &= (l_2 \sin(u_2(k)) + l_3 \sin(u_2(k) + u_3(k)) \cos(u_1(k)) \\ y(k+1) &= (l_2 \sin(u_2(k)) + l_3 \sin(u_2(k) + u_3(k)) \sin(u_1(k)) \\ z(k+1) &= l_1 + l_2 \cos(u_2(k)) + l_3 \cos(u_2(k) + u_3(k)) \end{aligned} \quad (14)$$

We take partial derivation of equation (14) to have the equivalent-dynamic-linearization model:

$$\Delta \mathbf{y}(k+1) = \begin{bmatrix} \Delta x(k+1) \\ \Delta y(k+1) \\ \Delta z(k+1) \end{bmatrix} = \boldsymbol{\Phi}(k) \begin{bmatrix} \Delta u_1(k) \\ \Delta u_2(k) \\ \Delta u_3(k) \end{bmatrix} \quad (15)$$

where $\boldsymbol{\Phi}(k)$ represents the Jacobian matrix. The desired output trajectory is considered as a helical curve:

$$\begin{aligned} x^*(k) &= 4 + 3 \sin(\pi k / 50) \\ y^*(k) &= 3 \cos(\pi k / 50) \\ z^*(k) &= 5 + k / 200 \end{aligned} \quad 1 \leq k \leq 800$$

The initial values are $[x(1), y(1), z(1)] = 0$, $u_1(1) = u_2(1) = u_3(1) = 0$, nevertheless these initial settings do not suffice the actual forward kinematic of robot. The initial controller parameter is $\boldsymbol{\lambda} = \text{diag}(\lambda, \dots, \lambda)$, $\lambda = 2$.

In order to remove the static error and to make sure the system stable, we applied the MFAC controller with $L_y = 0$, $L_u = 1$:

$$\Delta \mathbf{u}(k) = [\boldsymbol{\Phi}^T(k) \boldsymbol{\Phi}(k) + \lambda(k) \mathbf{I}]^{-1} \boldsymbol{\Phi}^T(k) [\mathbf{y}^*(k+1) - \mathbf{y}(k)] \quad (16)$$

If $\|\mathbf{y}^*(k+1) - \mathbf{y}(k)\|_2 > 1$

$$\lambda(k) = 1.2 \cdot \lambda(k-1)$$

else $\lambda(k) = \lambda(k-1) / 1.02$

where $\mathbf{y}^*(k+1) = [x^*(k+1), y^*(k+1), z^*(k+1)]^T$ is the desired trajectory, $\|\bullet\|_2$ is the norm of the vector, and the current position is $\mathbf{y}(k) = [x(k), y(k), z(k)]^T$.

The outputs of the system controlled by MFAC and the value of controller parameter λ are shown in Fig. 2. The control inputs are shown in Fig. 3. Fig. 4 shows the time-varying elements in $\boldsymbol{\Phi}(k)$ of MFAC.

Since the initial value of inputs and outputs of the system violates the kinematic of robot, the beginning tracking performance is not well. Simultaneously, λ increases to enhance the robustness of the system. After the system is stable with the tracking error of the system lower than 1 at time of 27, λ decreases to guarantee the convergence of the tracking error.

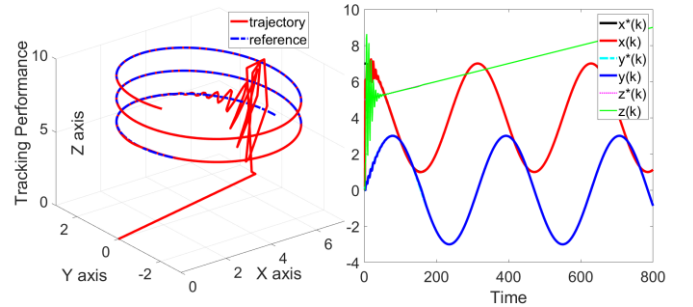


Fig. 2 Tracking performance

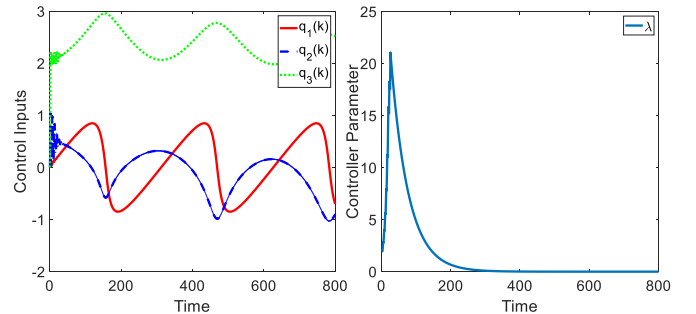


Fig. 3 Control inputs and controller parameter λ

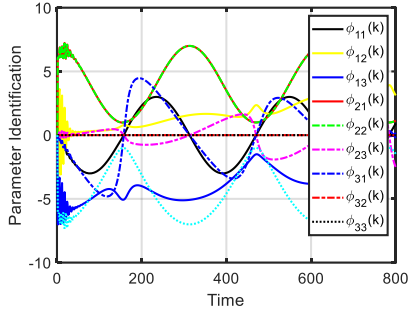


Fig. 4 Elements in $\Phi(k)$

In next example, we will show that the utilization of matrix $[\Phi^T(k)\Phi(k) + \lambda(k)I]^{-1}\Phi^T(k)$ instead of $\Phi^{-1}(k)$ makes the robot stay stable even near the singularities. For more details, please refer to the inverse kinematic code in ikine.m of MATLAB Robotics Toolbox which is applied in accordance with [8]-[10]. Additionally, the method in [8] can be regarded as a case of MFAC when $L_y = 0$, $L_u = 1$.

Example 2: A six dimensional industrial robot is shown in Fig. 5. Herein, we will design a simple yet useful controller for the industrial robot manipulator. The block diagram of the system is shown in Fig. 6.



Fig. 5 Robot manipulator

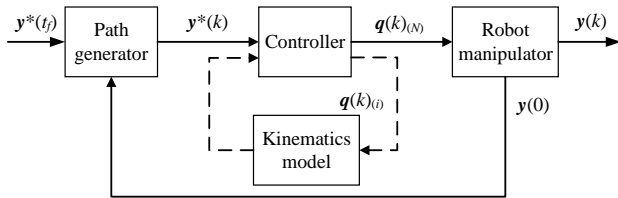


Fig. 6 Block diagram of the system

According to the manual, Table I gives the Denavit-Hartenberg parameters (link twist α_{i-1} , link length a_{i-1} , link offset d_i , and joint angle q_i) of the manipulator to calculate the frame in Cartesian-space.

TABLE I Denavit-Hartenberg parameters

| i | $\alpha_{i-1} / ^\circ$ | a_{i-1} / mm | d_i / mm | q_i |
|------|-------------------------|-----------------------|-------------------|-------|
| Base | 0 | 0 | 342 | 0 |
| 1 | 0 | 0 | 0 | q_1 |
| 2 | -90 | 40 | 0 | q_2 |
| 3 | 0 | 275 | 0 | q_3 |
| 4 | -90 | 25 | 280 | q_4 |
| 5 | 90 | 0 | 0 | q_5 |
| 6 | -90 | 0 | 0 | q_6 |
| Tool | 0 | 0 | 73 | 0 |

Part A: MFAC controller design for inverse kinematics solutions

Given the desired path point in desired trajectory (planned Cartesian-space paths) at path-planning time k is

$$\mathbf{y}^*(k) = [x^*(k), y^*(k), z^*(k), \alpha^*(k), \beta^*(k), \gamma^*(k)]^T \quad (17)$$

It is normal to choose the Cartesian-space scheme for the linear spline with parabolic blends path in **Part B** of this example [10].

The corresponding desired frame can be described as

$$\mathbf{T}^*(k) = \begin{pmatrix} \mathbf{A}^*(k) & \mathbf{p}^*(k) \\ \mathbf{0}_{3 \times 1} & 1 \end{pmatrix} \quad (18)$$

where

$$\mathbf{A}^*(k) = \begin{bmatrix} t_{11}^*(k) & t_{12}^*(k) & t_{13}^*(k) \\ t_{21}^*(k) & t_{22}^*(k) & t_{23}^*(k) \\ t_{31}^*(k) & t_{32}^*(k) & t_{33}^*(k) \end{bmatrix} \quad (19)$$

is the desired rotation matrix and

$$\mathbf{p}^*(k) = [x^*(k), y^*(k), z^*(k)]^T \quad (20)$$

is the desired position vector.

$$t_{11}^*(k) = c\beta^*(k)c\gamma^*(k)$$

$$t_{12}^*(k) = c\gamma^*(k)s\alpha^*(k)s\beta^*(k) - c\alpha^*(k)s\gamma^*(k)$$

$$t_{13}^*(k) = s\alpha^*(k)s\gamma^*(k) + c\alpha^*(k)c\gamma^*(k)s\beta^*(k)$$

$$t_{21}^*(k) = c\beta^*(k)s\gamma^*(k)$$

$$t_{22}^*(k) = c\alpha^*(k)c\gamma^*(k) + s\alpha^*(k)s\gamma^*(k)s\beta^*(k)$$

$$t_{23}^*(k) = c\alpha^*(k)s\beta^*(k)s\gamma^*(k) - c\gamma^*(k)s\alpha^*(k)$$

$$t_{31}^*(k) = -s\beta^*(k), \quad t_{32}^*(k) = c\beta^*(k)s\alpha^*(k)$$

$$t_{13}^*(k) = c\alpha^*(k)c\beta^*(k)$$

where $c\bullet$ is shorthand for $\cos(\bullet)$, $s\bullet$ for $\sin(\bullet)$, and so on.

The calculated robot frame at the i -th iteration for solving the inverse kinematics concerning the desired path point $\mathbf{y}^*(k+1)$ is described by

$$\mathbf{T}(k)_{(i)} = \begin{bmatrix} t(k)_{11(i)} & t(k)_{12(i)} & t(k)_{13(i)} & x(k)_{(i)} \\ t(k)_{21(i)} & t(k)_{22(i)} & t(k)_{23(i)} & y(k)_{(i)} \\ t(k)_{31(i)} & t(k)_{32(i)} & t(k)_{33(i)} & z(k)_{(i)} \\ 0 & 0 & 0 & 1 \end{bmatrix} \quad (21)$$

Hence, the corresponding orientation matrix is

$$\mathbf{A}(k)_{(i)} = \begin{bmatrix} t(k)_{11(i)} & t(k)_{12(i)} & t(k)_{13(i)} \\ t(k)_{21(i)} & t(k)_{22(i)} & t(k)_{23(i)} \\ t(k)_{31(i)} & t(k)_{32(i)} & t(k)_{33(i)} \end{bmatrix} \quad (22)$$

Then the desired orientation matrix relative to the calculated orientation matrix of manipulator at the i -th iteration is obtained

$$\begin{aligned} \mathbf{D}(k)_{(i)} &= \begin{bmatrix} d(k)_{11(i)} & d(k)_{12(i)} & d(k)_{13(i)} \\ d(k)_{21(i)} & d(k)_{22(i)} & d(k)_{23(i)} \\ d(k)_{31(i)} & d(k)_{32(i)} & d(k)_{33(i)} \end{bmatrix} \\ &= \mathbf{A}^*(k+1)(\mathbf{A}(k)_{(i)})^{-1} \end{aligned} \quad (23)$$

Now, we convert the orientation matrix into equivalent angle-axis representation to calculate the tracking error of the Euler angles vector. The angle is

$$\theta(k)_{(i)} = \arccos\left(\frac{d(k)_{11(i)} + d(k)_{11(i)} + d(k)_{33(i)} - 1}{2}\right) \quad (24)$$

The equivalent axis of a finite rotation is

$$\hat{\mathbf{K}}(k)_{(i)} = \begin{pmatrix} d(k)_{32(i)} - d(k)_{23(i)} \\ d(k)_{13(i)} - d(k)_{31(i)} \\ d(k)_{21(i)} - d(k)_{12(i)} \end{pmatrix} / 2 \sin \theta(k)_{(i)} \quad (25)$$

Then the relative rotational Euler angles vector is calculated by

$$\begin{bmatrix} \alpha^*(k+1) - \alpha(k)_{(i)} \\ \beta^*(k+1) - \beta(k)_{(i)} \\ \gamma^*(k+1) - \gamma(k)_{(i)} \end{bmatrix} = \hat{\mathbf{K}}(k)_{(i)} \theta(k)_{(i)} \quad (26)$$

The control law is

$$\begin{aligned} \Delta \mathbf{q}(k)_{(i)} &= [\Phi^T(k)_{(i)} \Phi(k)_{(i)} + \lambda(k)_{(i)}]^{-1} \Phi^T(k)_{(i)} [(y^*(k+1) - y(k)_{(i)})] \\ &= [\Phi^T(k)_{(i)} \Phi(k)_{(i)} + \lambda(k)_{(i)}]^{-1} \Phi^T(k)_{(i)} [x^*(k+1) - x(k)_{(i)}, \\ &\quad y^*(k+1) - y(k)_{(i)}, z^*(k+1) - z(k)_{(i)}, \alpha^*(k+1) - \alpha(k)_{(i)}, \\ &\quad \beta^*(k+1) - \beta(k)_{(i)}, \gamma^*(k+1) - \gamma(k)_{(i)}]^T \end{aligned} \quad (27)$$

We adjust the controller parameters in accordance with the following lookup table

$$\lambda(k)_{(i+1)} = \begin{cases} 0, & \text{if } \text{cond}(J(k)_{(i)}) < 5000 \\ 0.05 & \text{if } 5000 \leq \text{cond}(J(k)_{(i)}) < 20000 \\ 0.1 & \text{if } \text{cond}(J(k)_{(i)}) \geq 20000 \end{cases} \quad (28)$$

The joint angle vector of manipulator at the i -th iteration is

$$\mathbf{q}(k)_{(i)} = \mathbf{q}(k)_{(i-1)} + \Delta \mathbf{q}(k)_{(i)} \quad (29)$$

According to the robot kinematics, we can transform $\mathbf{q}(k)_{(i)}$ into

$$\mathbf{y}(k)_{(i+1)} = [x(k)_{(i+1)}, y(k)_{(i+1)}, z(k)_{(i+1)}, \alpha(k)_{(i+1)}, \beta(k)_{(i+1)}, \gamma(k)_{(i+1)}]^T \quad (30)$$

which can be transformed into (21) for the $(i+1)$ -th iteration directly. And the Jacobian matrix $\Phi(k)_{(i+1)}$ is only decided by $\mathbf{q}(k)_{(i)}$. Then (21)-(30) forms a closed-loop to calculate the inverse kinematics solution for the desired path point $\mathbf{y}^*(k+1)$.

In this example, the maximum number of iterations is limited to 30.

Part B: Path generator

Herein, the generation of Cartesian-space paths is designed for the linear spline with quantic blends path.

We plan the straight-line-path that begins with the initial frame of the manipulator $[x(0), y(0), z(0), \alpha(0), \beta(0), \gamma(0)]^T$ and ends at the goal frame $[x^*(t_f), y^*(t_f), z^*(t_f), \alpha^*(t_f), \beta^*(t_f), \gamma^*(t_f)]^T$. Thus, the initial position vector is written as $\mathbf{p}(0) = [x(0), y(0), z(0)]^T$ and the goal position vector is written as $\mathbf{p}^*(t_f) = [x^*(t_f), y^*(t_f), z^*(t_f)]^T$.

A quantic polynomial is used for Cartesian-straight-line-motion scheme

$$S_1(t) = a_0 + a_1 t + a_2 t^2 + a_3 t^3 + a_4 t^4 + a_5 t^5, \quad 0 \leq t \leq t_f \quad (31)$$

The coefficients a_i ($i=1, \dots, 5$) are specified by the constraints: initial velocity $\dot{\mathbf{p}}(0)$, initial acceleration $\ddot{\mathbf{p}}(0)$, goal position

$S_1(t_f)$ ($\mathbf{p}^*(t_f)$), goal velocity $\dot{\mathbf{p}}^*(t_f)$ and goal acceleration $\ddot{\mathbf{p}}^*(t_f)$ at the final time t_f . The solution of a_i is

$$\begin{aligned} a_0 &= 0 \\ a_1 &= \|\dot{\mathbf{p}}(0)\|_2 \\ a_2 &= \|\ddot{\mathbf{p}}(0)\|_2 / 2 \\ a_3 &= \frac{20S_1(t_f) - (8\|\dot{\mathbf{p}}^*(t_f)\|_2 + 12\|\dot{\mathbf{p}}(0)\|_2)t_f - (3\|\ddot{\mathbf{p}}(0)\|_2 - \|\ddot{\mathbf{p}}^*(t_f)\|_2)t_f^2}{2t_f^3} \\ a_4 &= \frac{-30S_1(t_f) - (14\|\dot{\mathbf{p}}^*(t_f)\|_2 + 16\|\dot{\mathbf{p}}(0)\|_2)t_f + (3\|\ddot{\mathbf{p}}(0)\|_2 - 2\|\ddot{\mathbf{p}}^*(t_f)\|_2)t_f^2}{2t_f^4} \\ a_5 &= \frac{12S_1(t_f) - 6(\|\dot{\mathbf{p}}^*(t_f)\|_2 + \|\dot{\mathbf{p}}(0)\|_2)t_f - (\|\ddot{\mathbf{p}}(0)\|_2 - \|\ddot{\mathbf{p}}^*(t_f)\|_2)t_f^2}{2t_f^5} \end{aligned} \quad (32)$$

Then the positional trajectory at path-planning time k , i.e. (21), is calculated by

$$\mathbf{p}^*(k) = \mathbf{p}(0) + \frac{\mathbf{p}^*(t_f) - \mathbf{p}(0)}{\|\mathbf{p}^*(t_f) - \mathbf{p}(0)\|_2} \cdot S_1(t) + \mathbf{p}(0) \quad (33)$$

where $t = kT_0$ and T_0 is the implementation period of the manipulator.

We know that the initial X-Y-Z Euler angle vector is $\boldsymbol{\Theta}(0) = [\alpha(0), \beta(0), \gamma(0)]^T$ and the goal X-Y-Z Euler angle vector is $\boldsymbol{\Theta}(t_f) = [\alpha^*(t_f), \beta^*(t_f), \gamma^*(t_f)]^T$.

We convert the goal X-Y-Z Euler angle vector into unit quaternion (Euler parameters):

$$\begin{aligned} \boldsymbol{\Pi}^*(t_f) &= [\varepsilon_1(t_f) \quad \varepsilon_2(t_f) \quad \varepsilon_3(t_f) \quad \varepsilon_4(t_f)]^T \\ &= \begin{bmatrix} s \frac{\alpha^*(t_f)}{2} c \frac{\beta^*(t_f)}{2} c \frac{\gamma^*(t_f)}{2} - c \frac{\alpha^*(t_f)}{2} s \frac{\beta^*(t_f)}{2} s \frac{\gamma^*(t_f)}{2} \\ c \frac{\alpha^*(t_f)}{2} s \frac{\beta^*(t_f)}{2} c \frac{\gamma^*(t_f)}{2} + s \frac{\alpha^*(t_f)}{2} c \frac{\beta^*(t_f)}{2} s \frac{\gamma^*(t_f)}{2} \\ c \frac{\alpha^*(t_f)}{2} c \frac{\beta^*(t_f)}{2} s \frac{\gamma^*(t_f)}{2} + s \frac{\alpha^*(t_f)}{2} s \frac{\beta^*(t_f)}{2} c \frac{\gamma^*(t_f)}{2} \\ c \frac{\alpha^*(t_f)}{2} c \frac{\beta^*(t_f)}{2} c \frac{\gamma^*(t_f)}{2} + s \frac{\alpha^*(t_f)}{2} s \frac{\beta^*(t_f)}{2} s \frac{\gamma^*(t_f)}{2} \end{bmatrix} \end{aligned} \quad (34)$$

Similarly, we can convert $\boldsymbol{\Theta}(0)$ into quaternion

$$\boldsymbol{\Pi}(0) = [\varepsilon_1(0), \varepsilon_2(0), \varepsilon_3(0), \varepsilon_4(0)]^T.$$

The length of path is

$$S_2(t_f) = \left\| 2\boldsymbol{\Pi}(0) \log(\boldsymbol{\Pi}^{-1}(0)\boldsymbol{\Pi}^*(t_f))\boldsymbol{\Pi}^{-1}(0) \right\|_2 \quad (35)$$

Similarly, the quantic polynomial is used for Cartesian-straight-line-motion scheme

$$S_2(t) = b_0 + b_1 t + b_2 t^2 + b_3 t^3 + b_4 t^4 + b_5 t^5, \quad t \leq t_f \quad (36)$$

Similar to (33), b_i ($i=1, \dots, 5$) are specified by the constraints:

$$\boldsymbol{\Pi}(0), \dot{\boldsymbol{\Pi}}(0), \ddot{\boldsymbol{\Pi}}(0), S(t_f), \dot{\boldsymbol{\Pi}}^*(t_f) \text{ and } \ddot{\boldsymbol{\Pi}}^*(t_f).$$

Define

$$[\bar{\varepsilon}_1 \quad \bar{\varepsilon}_2 \quad \bar{\varepsilon}_3 \quad \bar{\varepsilon}_4]^T = \boldsymbol{\Pi}^{-1}(0)\boldsymbol{\Pi}^*(t_f) \quad (37)$$

We obtain the quaternion argument

$$a = \arccos \bar{\varepsilon}_4 \quad (38)$$

Then we have the desired orientation at path-planning time k

$$\begin{aligned}\mathbf{H}(k) &= [\varepsilon_1(k) \ \varepsilon_2(k) \ \varepsilon_3(k) \ \varepsilon_4(k)]^T \\ &= \mathbf{H}(0) [\mathbf{H}^{-1}(0) \mathbf{H}^*(t_f)]^\tau, \quad \tau = \frac{S_2(t)}{S_2(t_f)}\end{aligned}\quad (39)$$

where

$$\begin{aligned}[\mathbf{H}^{-1}(0) \mathbf{H}^*(t_f)]^\tau &= \exp(\tau \log(\mathbf{H}^{-1}(0) \mathbf{H}^*(t_f))) \\ &= \exp([0, a\tau(\bar{\varepsilon}_1/sa \ \bar{\varepsilon}_2/sa \ \bar{\varepsilon}_3/sa)]) \\ &= \begin{bmatrix} \bar{\varepsilon}_1 s(a S_2(t)/S_2(t_f))/sa \\ \bar{\varepsilon}_2 s(a S_2(t)/S_2(t_f))/sa \\ \bar{\varepsilon}_3 s(a S_2(t)/S_2(t_f))/sa \\ c(a S_2(t)/S_2(t_f)) \end{bmatrix}, \quad t = kT_0\end{aligned}\quad (40)$$

and $\exp(\bullet)$ represents exponential operation, $\log(\bullet)$ represents logarithmic operation. We convert (39) into X-Y-Z Euler angle vector

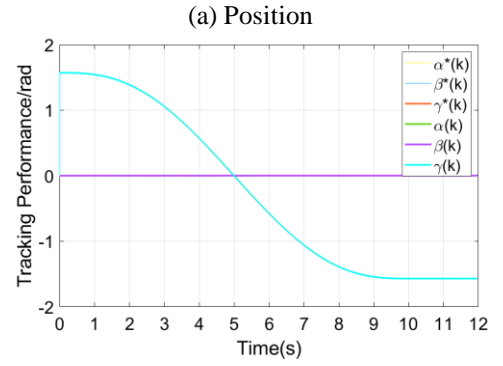
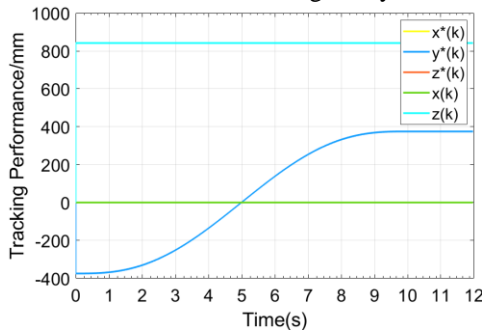
$$\begin{aligned}\boldsymbol{\Theta}^*(k) &= [\alpha^*(k), \beta^*(k), \gamma^*(k)]^T \\ &= \begin{bmatrix} \arctan\left(\frac{2(\varepsilon_4(k)\varepsilon_1(k) + \varepsilon_2(k)\varepsilon_3(k))}{1 - 2(\varepsilon_1^2(k) + \varepsilon_2^2(k))}\right) \\ \arcsin\left(\frac{2(\varepsilon_4(k)\varepsilon_2(k) - \varepsilon_3(k)\varepsilon_1(k))}{1 - 2(\varepsilon_1^2(k) + \varepsilon_2^2(k))}\right) \\ \arctan\left(\frac{2(\varepsilon_4(k)\varepsilon_3(k) + \varepsilon_1(k)\varepsilon_2(k))}{1 - 2(\varepsilon_2^2(k) + \varepsilon_3^2(k))}\right) \end{bmatrix}\end{aligned}\quad (41)$$

which can be transformed into (19) directly. We finish the design of the desired trajectory in (17).

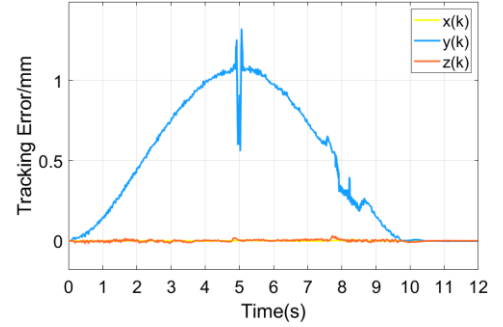
Part C: Test MFAC control law

Herein, The MFAC in Part A is tested by tracking the trajectory defined in the task space. The beginning joint angle vector of manipulator is $\mathbf{A} [-\pi/2, 0, 0, 0, -\pi/2, 0]^T$. The path generator in Part B is used to plan a straight-line path in Cartesian-space from \mathbf{A} to $\mathbf{C} [\pi/2, 0, 0, 0, -\pi/2, 0]^T$. As the consequence, there will be two singular points \mathbf{B} and \mathbf{C} in the trajectory. The manipulator frames \mathbf{A} , \mathbf{B} and \mathbf{C} are marked in Fig. 5. Fig. 7 shows the tracking performance of the manipulator and Fig. 8 shows the corresponding tracking error. Fig. 9 shows the measured joint angles. Fig. 10 shows a part of elements in $\boldsymbol{\Phi}(k)$. Fig. 11 shows condition number and Fig. 12 shows the controller parameter λ . Fig. 13 shows the iteration count.

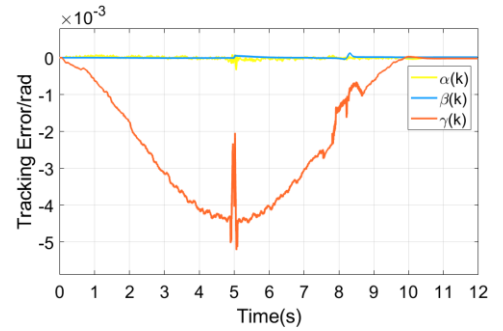
From Fig. 11, we know that the PJM is ill-conditioned at the time of 4.997s and 8.229s. With the higher controller parameter λ in Fig. 12, the system does not diverge, but the iteration count reaches the maximum value 30. From Fig. 8, we know that the controller induces the biggest position errors of manipulator within 1.4mm and the biggest orientation errors within 6×10^{-3} rad when the robot moves near the singularity.



(b) Orientation
Fig. 7 Tracking performance



(a) Position



(b) Orientation

Fig. 8 Tracking error

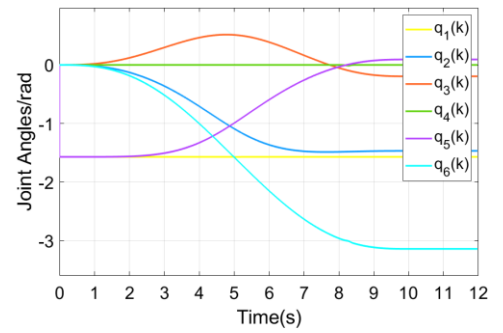


Fig. 9 Joint angles

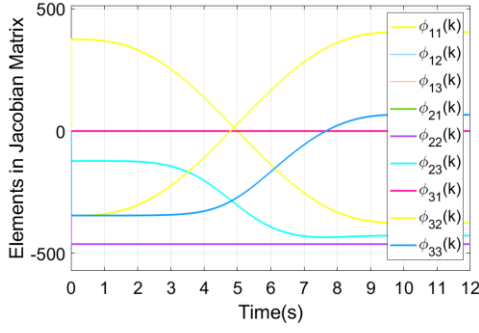
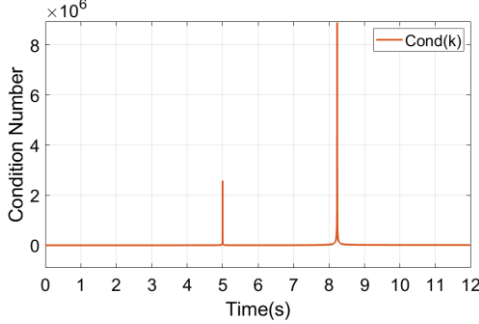
Fig. 10 Elements in $\Phi(k)$ 

Fig. 11 Condition number in iterations

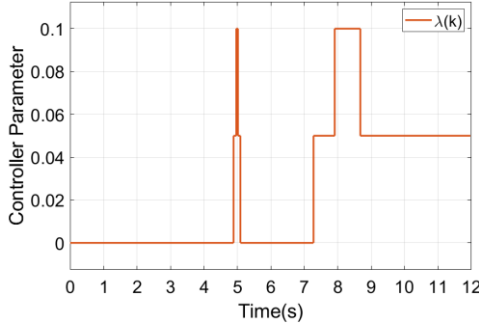
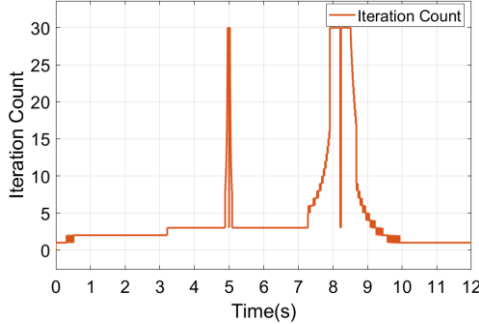
Fig. 12 Controller parameter λ 

Fig. 13 Iteration count

V. CONCLUSION

In this brief, we have figured out that some MFAC methods are not studied in a right way. To this end, a kind of MFAC for a family of multivariable nonlinear systems is redesigned in this brief and then the stability of the system and the chosen parameter λ are analyzed by the closed-loop function. At last, we exhibit an appropriate and successful application in the robotic manipulator control.

APPENDIX

Proof of Theorem 1

Proof: Case 1: $0 \leq L_y \leq n_y$ and $1 \leq L_u \leq n_u$

From (1), we have

$$\begin{aligned} \Delta \mathbf{y}(k+1) = & \mathbf{f}(\mathbf{y}(k), \dots, \mathbf{y}(k-L_y+1), \mathbf{y}(k-L_y), \dots, \mathbf{y}(k-n_y), \mathbf{u}(k), \\ & \dots, \mathbf{u}(k-L_u+1), \mathbf{u}(k-L_u), \dots, \mathbf{u}(k-n_u)) \\ & - \mathbf{f}(\mathbf{y}(k-1), \dots, \mathbf{y}(k-L_y), \mathbf{y}(k-L_y-1), \dots, \mathbf{y}(k-n_y), \mathbf{u}(k-1), \\ & \dots, \mathbf{u}(k-L_u), \mathbf{u}(k-L_u-1), \dots, \mathbf{u}(k-n_u)) \\ & + \mathbf{f}(\mathbf{y}(k-1), \dots, \mathbf{y}(k-L_y), \mathbf{y}(k-L_y), \dots, \mathbf{y}(k-n_y), \mathbf{u}(k-1), \\ & \dots, \mathbf{u}(k-L_u), \mathbf{u}(k-L_u), \dots, \mathbf{u}(k-n_u)) \\ & - \mathbf{f}(\mathbf{y}(k-1), \dots, \mathbf{y}(k-L_y), \mathbf{y}(k-L_y-1), \dots, \mathbf{y}(k-n_y-1), \\ & \mathbf{u}(k-1), \dots, \mathbf{u}(k-L_u), \mathbf{u}(k-L_u-1), \dots, \mathbf{u}(k-n_u-1)) \end{aligned} \quad (42)$$

On the basis of *Assumption 1* and the definition of differentiability in [11], (42) becomes

$$\begin{aligned} \Delta \mathbf{y}(k+1) = & \frac{\partial \mathbf{f}}{\partial \mathbf{y}^T(k)} \Delta \mathbf{y}(k) + \dots + \frac{\partial \mathbf{f}}{\partial \mathbf{y}^T(k-L_y+1)} \Delta \mathbf{y}(k-L_y+1) \\ & + \frac{\partial \mathbf{f}}{\partial \mathbf{u}^T(k)} \Delta \mathbf{u}(k) + \dots + \frac{\partial \mathbf{f}}{\partial \mathbf{u}^T(k-L_u+1)} \Delta \mathbf{u}(k-L_u+1) \\ & + \varepsilon_1 \Delta \mathbf{y}(k) + \dots + \varepsilon_{L_y} \Delta \mathbf{y}(k-L_y+1) + \varepsilon_{L_y+1} \Delta \mathbf{u}(k) + \dots \\ & + \varepsilon_{L_y+L_u} \Delta \mathbf{u}(k-L_u+1) + \boldsymbol{\psi}(k) \end{aligned} \quad (43)$$

or

$$\begin{aligned} \Delta \mathbf{y}(k+1) = & \left. \frac{\partial \mathbf{f}}{\partial \mathbf{y}^T(k)} \right|_{k=k-1} \Delta \mathbf{y}(k) + \dots + \left. \frac{\partial \mathbf{f}}{\partial \mathbf{y}^T(k-L_y+1)} \right|_{k=k-1} \Delta \mathbf{y}(k-L_y+1) \\ & + \left. \frac{\partial \mathbf{f}}{\partial \mathbf{u}^T(k)} \right|_{k=k-1} \Delta \mathbf{u}(k) + \dots + \left. \frac{\partial \mathbf{f}}{\partial \mathbf{u}^T(k-L_u+1)} \right|_{k=k-1} \Delta \mathbf{u}(k-L_u+1) \\ & + \varepsilon_1 \Delta \mathbf{y}(k) + \dots + \varepsilon_{L_y} \Delta \mathbf{y}(k-L_y+1) + \varepsilon_{L_y+1} \Delta \mathbf{u}(k) + \dots \\ & + \varepsilon_{L_y+L_u} \Delta \mathbf{u}(k-L_u+1) + \boldsymbol{\psi}(k) \end{aligned} \quad (44)$$

where

$$\begin{aligned} \boldsymbol{\psi}(k) \triangleq & \mathbf{f}(\mathbf{y}(k-1), \dots, \mathbf{y}(k-L_y), \mathbf{y}(k-L_y), \dots, \mathbf{y}(k-n_y), \\ & \mathbf{u}(k-1), \dots, \mathbf{u}(k-L_u), \mathbf{u}(k-L_u), \dots, \mathbf{u}(k-n_u)) \\ & - \mathbf{f}(\mathbf{y}(k-1), \dots, \mathbf{y}(k-L_y), \mathbf{y}(k-L_y-1), \dots, \mathbf{y}(k-n_y-1), \\ & \mathbf{u}(k-1), \dots, \mathbf{u}(k-L_u), \mathbf{u}(k-L_u-1), \dots, \mathbf{u}(k-n_u-1)) \end{aligned} \quad (45)$$

$$\frac{\partial \mathbf{f}}{\partial \mathbf{y}^T(k-i)} = \begin{bmatrix} \frac{\partial f_1}{\partial y_1(k-i)} & \frac{\partial f_1}{\partial y_2(k-i)} & \dots & \frac{\partial f_1}{\partial y_{M_y}(k-i)} \\ \frac{\partial f_2}{\partial y_1(k-i)} & \frac{\partial f_2}{\partial y_2(k-i)} & \dots & \frac{\partial f_2}{\partial y_{M_y}(k-i)} \\ \vdots & \vdots & \ddots & \vdots \\ \frac{\partial f_{M_y}}{\partial y_1(k-i)} & \frac{\partial f_{M_y}}{\partial y_2(k-i)} & \dots & \frac{\partial f_{M_y}}{\partial y_{M_y}(k-i)} \end{bmatrix},$$

$$0 \leq i \leq L_y - 1,$$

$$\frac{\partial f}{\partial \mathbf{u}^T(k-j)} = \begin{bmatrix} \frac{\partial f_1}{\partial u_1(k-j)} & \frac{\partial f_1}{\partial u_2(k-j)} & \cdots & \frac{\partial f_1}{\partial u_{Mu}(k-j)} \\ \frac{\partial f_2}{\partial u_1(k-i)} & \frac{\partial f_2}{\partial u_2(k-i)} & \cdots & \frac{\partial f_2}{\partial u_{Mu}(k-j)} \\ \vdots & \vdots & \ddots & \vdots \\ \frac{\partial f_{My}}{\partial u_1(k-i)} & \frac{\partial f_{My}}{\partial u_2(k-i)} & \cdots & \frac{\partial f_{My}}{\partial u_{Mu}(k-j)} \end{bmatrix},$$

$0 \leq j \leq L_u - 1$ denote the partial derivative of $f(\cdots)$ with respect to the $(i+1)$ -th vector, the (n_y+2+j) -th vector at some point within

$$[\mathbf{y}(k), \cdots, \mathbf{y}(k-L_y+1), \mathbf{y}(k-L_y), \cdots, \mathbf{y}(k-n_y), \mathbf{u}(k), \cdots, \mathbf{u}(k-L_u+1), \mathbf{u}(k-L_u), \cdots, \mathbf{u}(k-n_u)]$$

and

$$[\mathbf{y}(k-1), \cdots, \mathbf{y}(k-L_y), \mathbf{y}(k-L_y), \cdots, \mathbf{y}(k-n_y), \mathbf{u}(k-1), \cdots, \mathbf{u}(k-L_u), \mathbf{u}(k-L_u), \cdots, \mathbf{u}(k-n_u)]$$

respectively. And $\varepsilon_1, \cdots, \varepsilon_{L_y+L_u}$ are functions that depend only on $\Delta \mathbf{y}(k), \cdots, \Delta \mathbf{y}(k-L_y+1), \Delta \mathbf{u}(k), \cdots, \Delta \mathbf{u}(k-L_u+1)$, with $(\varepsilon_1, \cdots, \varepsilon_{L_y+L_u}) \rightarrow (\mathbf{0}, \cdots, \mathbf{0})$ when $(\Delta \mathbf{y}(k), \cdots, \Delta \mathbf{y}(k-L_y+1), \Delta \mathbf{u}(k), \cdots, \Delta \mathbf{u}(k-L_u+1)) \rightarrow (\mathbf{0}, \cdots, \mathbf{0})$.

Both (43) and (44) satisfy the definition of differentiability. Because of space limitations, this brief uses (43) in the proof to be consistent with [3] and is based on (44) in experiments.

We consider the following equation with the vector $\boldsymbol{\eta}(k)$ for each time k :

$$\boldsymbol{\psi}(k) = \boldsymbol{\eta}^T(k) \Delta \mathbf{H}(k) \quad (46)$$

Owing to $\|\Delta \mathbf{H}(k)\| \neq 0$, (46) must have at least one solution $\boldsymbol{\eta}_0^T(k)$. Let

$$\begin{aligned} \boldsymbol{\phi}_L^T(k) = & \boldsymbol{\eta}_0^T(k) + \left[\frac{\partial f}{\partial \mathbf{y}^T(k)} + \varepsilon_1, \cdots, \frac{\partial f}{\partial \mathbf{y}^T(k-L_y+1)} + \varepsilon_{L_y}, \right. \\ & \left. \frac{\partial f}{\partial \mathbf{u}^T(k)} + \varepsilon_{L_y+1}, \cdots, \frac{\partial f}{\partial \mathbf{u}^T(k-L_u+1)} + \varepsilon_{L_y+L_u} \right] \end{aligned} \quad (47)$$

Then (43) can be described as follow:

$$\Delta \mathbf{y}(k+1) = \boldsymbol{\phi}_L^T(k) \Delta \mathbf{H}(k) \quad (48)$$

Case 2: $L_y = n_y + 1$ and $L_u = n_u + 1$

On the basis of *Assumption 1* and the definition of differentiability in [11], (1) becomes

$$\begin{aligned} \Delta \mathbf{y}(k+1) = & \frac{\partial f}{\partial \mathbf{y}^T(k)} \Delta \mathbf{y}(k) + \cdots + \frac{\partial f}{\partial \mathbf{y}^T(k-n_y)} \Delta \mathbf{y}(k-n_y) \\ & + \frac{\partial f}{\partial \mathbf{u}^T(k)} \Delta \mathbf{u}(k) + \cdots + \frac{\partial f}{\partial \mathbf{u}^T(k-n_u)} \Delta \mathbf{u}(k-n_u) \quad (49) \\ & + \varepsilon_1 \Delta \mathbf{y}(k) + \cdots + \varepsilon_{L_y} \Delta \mathbf{y}(k-n_y) + \varepsilon_{L_y+1} \Delta \mathbf{u}(k) + \cdots \\ & + \varepsilon_{L_y+L_u} \Delta \mathbf{u}(k-n_u) \end{aligned}$$

and we let

$$\begin{aligned} \boldsymbol{\phi}_L^T(k) = & \left[\frac{\partial f}{\partial \mathbf{y}^T(k)} + \varepsilon_1, \cdots, \frac{\partial f}{\partial \mathbf{y}^T(k-n_y)} + \varepsilon_{L_y}, \right. \\ & \left. \frac{\partial f}{\partial \mathbf{u}^T(k)} + \varepsilon_{L_y+1}, \cdots, \frac{\partial f}{\partial \mathbf{u}^T(k-n_u)} + \varepsilon_{L_y+L_u} \right] \end{aligned} \quad (50)$$

to describe (49) as follow:

$$\Delta \mathbf{y}(k+1) = \boldsymbol{\phi}_L^T(k) \Delta \mathbf{H}(k) \quad (51)$$

, with $(\varepsilon_1, \cdots, \varepsilon_{L_y+L_u}) \rightarrow (\mathbf{0}, \cdots, \mathbf{0})$, i.e., $\boldsymbol{\phi}_L^T(k) \rightarrow [\frac{\partial f}{\partial \mathbf{y}^T(k)}, \cdots, \frac{\partial f}{\partial \mathbf{y}^T(k-n_y)}, \frac{\partial f}{\partial \mathbf{u}^T(k)}, \cdots, \frac{\partial f}{\partial \mathbf{u}^T(k-n_u)}]$ in nonlinear systems, when $(\Delta \mathbf{y}(k), \cdots, \Delta \mathbf{y}(k-n_y), \Delta \mathbf{u}(k), \cdots, \Delta \mathbf{u}(k-n_u)) \rightarrow (\mathbf{0}, \cdots, \mathbf{0})$.

As to linear systems, we will always have $\boldsymbol{\phi}_L^T(k) = [\frac{\partial f}{\partial \mathbf{y}^T(k)}, \cdots,$

$\frac{\partial f}{\partial \mathbf{y}^T(k-n_y)}, \frac{\partial f}{\partial \mathbf{u}^T(k)}, \cdots, \frac{\partial f}{\partial \mathbf{u}^T(k-n_u)}]$, no matter what $(\Delta \mathbf{y}(k), \cdots, \Delta \mathbf{y}(k-n_y), \Delta \mathbf{u}(k), \cdots, \Delta \mathbf{u}(k-n_u))$ is.

Case 3: $L_y > n_y + 1$ and $L_u > n_u + 1$

On the basis of *Assumption 1* and the definition of differentiability in [11], (1) becomes

$$\begin{aligned} \Delta \mathbf{y}(k+1) = & \frac{\partial f}{\partial \mathbf{y}^T(k)} \Delta \mathbf{y}(k) + \cdots + \frac{\partial f}{\partial \mathbf{y}^T(k-n_y)} \Delta \mathbf{y}(k-n_y) \\ & + \frac{\partial f}{\partial \mathbf{u}^T(k)} \Delta \mathbf{u}(k) + \cdots + \frac{\partial f}{\partial \mathbf{u}^T(k-n_u)} \Delta \mathbf{u}(k-n_u) \\ & + \varepsilon_1 \Delta \mathbf{y}(k) + \cdots + \varepsilon_{n_y+1} \Delta \mathbf{y}(k-n_y) + \varepsilon_{L_y+1} \Delta \mathbf{u}(k) + \cdots \\ & + \varepsilon_{L_y+n_u+1} \Delta \mathbf{u}(k-n_u) \end{aligned} \quad (52)$$

Define

$$\begin{aligned} \boldsymbol{\gamma}(k) = & \varepsilon_1 \Delta \mathbf{y}(k) + \cdots + \varepsilon_{n_y+1} \Delta \mathbf{y}(k-n_y) + \varepsilon_{L_y+1} \Delta \mathbf{u}(k) + \cdots \\ & + \varepsilon_{L_y+n_u+1} \Delta \mathbf{u}(k-n_u) \end{aligned} \quad (53)$$

We consider the following equation with the vector $\boldsymbol{\eta}(k)$ for each time k :

$$\boldsymbol{\gamma}(k) = \boldsymbol{\eta}^T(k) \Delta \mathbf{H}(k) \quad (54)$$

Owing to $\|\Delta \mathbf{H}(k)\| \neq 0$, (54) must have at least one solution $\boldsymbol{\eta}_0^T(k)$. Let

$$\begin{aligned} \boldsymbol{\phi}_L^T(k) = & \boldsymbol{\eta}_0^T(k) + \left[\frac{\partial f}{\partial \mathbf{y}^T(k)}, \cdots, \frac{\partial f}{\partial \mathbf{y}^T(k-n_y)}, \mathbf{0}, \cdots, \mathbf{0} \right. \\ & \left. \frac{\partial f}{\partial \mathbf{u}^T(k)}, \cdots, \frac{\partial f}{\partial \mathbf{u}^T(k-n_u)}, \mathbf{0}, \cdots, \mathbf{0} \right]^T \end{aligned} \quad (55)$$

Then (52) can be described as (48).

Case 4: $L_y \geq n_y + 1$ and $1 \leq L_u < n_u + 1$; $0 \leq L_y < n_y + 1$ and $L_u \geq n_u + 1$.

The proof of Case 4 is similar to the above process, we omit it. We finished the proof of *Theorem 1*.

REFERENCES

- [1] Hou Z S, Xiong S S. On Model Free Adaptive Control and its Stability Analysis[J]. IEEE Transactions on Automatic Control, 2019, 64(11): 4555-4569.
- [2] Hou Z S, Jin S T, "A novel data-driven control approach for a class of discrete-time nonlinear systems[J]. IEEE Transaction on Control Systems Technology, 2011, 19(6): 1549-1558.
- [3] Hou Z S, Jin S T, Model Free Adaptive Control: Theory and Applications, CRC Press, Taylor and Francis Group, 2013

- [4] Hou Z S, Jin S T. Data-Driven Model-Free Adaptive Control for a Class of MIMO Nonlinear Discrete-Time Systems[J]. IEEE Transactions on Neural Networks, 2011, 22(12): 2173-2188.
- [5] Guo Y, Hou Z S, Liu S D, Jin S T. Data-Driven Model-Free Adaptive Predictive Control for a Class of MIMO Nonlinear Discrete-Time Systems With Stability Analysis[J]. IEEE Access, 2019: 102852-102866.
- [6] Chai T Y. Multivariable adaptive decoupling control and its application [M]. Beijing: Science Press, 2001.
- [7] Chai T Y, Yue H. Adaptive Control [M]. Beijing: Tsinghua University Press, 2015.
- [8] Sugihara T. Solvability-Unconcerned Inverse Kinematics by the Levenberg-Marquardt Method[J]. IEEE Transactions on Robotics, 2011, 27(5):984-991.
- [9] Lynch K M, Park F C. Modern Robotics [M]. Cambridge University Press, 2017.
- [10] Craig J J. Introduction to Robotics: Mechanics and Control, Addison-Wesley, Boston, 2005.
- [11] Briggs W, Cochran L, Gillett B. Calculus [M]. Pearson, 2014.
- [a] Performance Analysis of Model-Free Adaptive Control
- [b] A New Model-Free Method for MIMO Systems and Discussion on Model-Free or Model-Based
- [c] Discussions on Inverse Kinematics based on Levenberg-Marquardt Method and Model-Free Adaptive (Predictive) Control